ISSN:3007-9640 DOI: https://doi.org/10.70114/acmsr.2025.3.1.P183

Vibration Reduction Performance of Multi-Particle Dampers Under Different Assumptions of Particle Motion States

Penggang Tian [1], Junlin Su [2] *, Kangning Liu [3], Yuliang Zhao [4], Jiantao Wang [5], Xuhong Huang [4]

[1] Future City Innovation Technology Co., Ltd., Shanxi Construction Engineering Holding Group, Xi'an 712000, China;

[2] Shandong Datong Construction Group Co., Ltd., Jinan 250109, China;

[3] SCEGC-XITU Joint Research Center for Future City Construction and Management Innovation, Xi'an 712000, China;

[4] School of Civil Engineering, Qingdao University of Technology, Qingdao 266520, China;

[5] Xian University of Architecture and Technology, School of Civil Engineering, Xi'an 710055, China

Abstract. Multi particle dampers have complex nonlinear characteristics. On the basis of analyzing the motion state of particles, different equivalent mechanics models have been proposed under different motion state assumptions. However, assumptions of mechanical models have a certain impact on the simulation result of vibration reduction performance. A full state equivalent single particle mechanics model was proposed on the basis of fully analyzing the motion state of a single particle. The method for numerical simulation of vibration reduction performance has also been proposed. The damping performance corresponding to different mechanical models was discussed subsequently under free vibration, harmonic, and seismic excitation. The results indicate that the assumption of motion state has a certain impact on the damping performance of multi particle dampers, especially considering the influence of acceleration.

Keywords: multi-particle damper; mechanic model; motion state; vibration reduction mechanism; parameter analysis

1. Introduction

The nonlinear characteristics of multi particle dampers (MPD) are a key issue that urgently needs to be addressed for their widespread application of MPD in engineering structures. To fully analyze the vibration reduction performance and mechanism of MPD, some related studies have been conducted through vibration table tests [1, 2], discrete element methods [3, 4], regression function methods [5, 6], or mechanical model methods [7]. Among them, the mechanical modelling method is not only able to reflect the motion state of the particle group, but also has better calculation efficiency and accuracy, which has better practical engineering application value.

The reasonable establishment of the mechanical models is of great significance for a correct understanding of the vibration reduction mechanism of MPD. Generally, the mechanical model of the MPD can be established by assuming collision models between particles and structures, as well as shear models between particles and the top of structures during their motion. The collision model explains the interaction between particles and structures during collisions (collision stage), such as collision damping and collision stiffness. The shear model explains the interaction between the particles and the top of the structure during motion (no-collision stage), such as friction. Up to now, collision modelling methods mainly include the contact element method [8] and the recovery coefficient method [9]. The contact element method interprets the collision relationship by introducing mechanical elements such as springs and dampers. The time-dependent effects of the collision can be considered. In contrast, the recovery coefficient method assumes that the collision occurs instantaneously. The absolute velocity of the system before and after the collision can be obtained through the defining equation of the recovery coefficient and the law of conservation of

ISSN:3007-9640 DOI: https://doi.org/10.70114/acmsr.2025.3.1.P183
momentum. The above two methods can basically explain the collision effects between particle groups and the structure for various types of MPD with an acceptable simulation accuracy. For shear models between particles and the top of structures, early mechanical models neglected the interactions between particles and the structure, leading to the development of the equivalent impact single particle (EISP) model [10], which considered only the collision effects between particles and the structure. Subsequently, considering the low-frequency characteristics of structural motion in civil engineering, Yan [11] incorporated the influence of rolling friction on the vibration reduction performance of MPD and proposed the equivalent single particle model considering rolling friction (EISP-RF). However, this model neglected the influence of rotational inertia on the damping effectiveness of the particles. Considered the effects of particle rolling and interactions among particles on inertial properties, Huang [12] have proposed an equivalent single particle model considering inertia (EISM). The above mechanical model explains the nonlinear properties of the MPD in some extent.

In summary, the existing collision models can explain the collision effects between particles and structures with accepteable accuracy, but the assumptions of the shear models are significantly different. To further clarify the effect of mechanical modelling assumptions on the vibration damping performance and mechanism, this study was carried out. Firstly, an equivalent whole status model (EWSM) was proposed on the basis of analysing the existing single-particle mechanical model and the real single-particle motion state. On this basis, a comparative analysis of the damping effect is carried out to discuss the influence of the mechanical model differences on the damping effect.

2. Equivalent Whole Status Model

2.1 Comparison of Existing Equivalent Single Particle Mechanics Models

Taking the single-degree-of-freedom structure (SDOF) as the controlled structure, the mechanical model of the MPD-SDOF corresponding to different assumptions of the shear model is shown in Fig. 1.

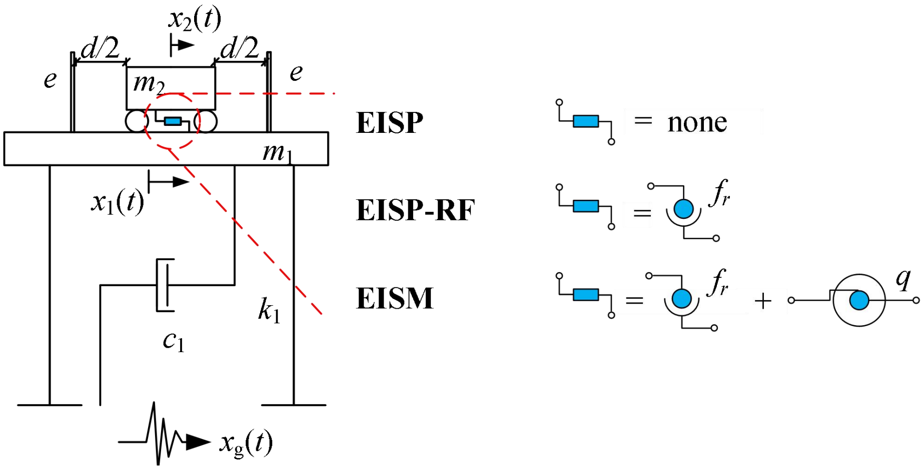

Fig. 1 Comparison of existing models

Where, m1 is the mass of the SDOF. m2 is the mass of the MPD. c1 is the damping coefficient of the SDOF. k1is the stiffness of the structure. xg (t) is the ground motion. x1, $\dot{x}1$ and $\ddot{x}1$ is the relative displacement, velocity, and acceleration of the SDOF respectively. x2, $\dot{x}2$ and $\ddot{x}2$ is the relative displacement, velocity, and acceleration of the MPD, respectively. d represents the collision gap between particles and strcture. e is the recovery coefficient. fr is the rolling friction coefficient. q is the inertia factor. When particles experience pure translational motion, q = 0. When particles experience pure rolling motion, q = 0.4m2, and when the interactions among particles are considered, q > 0.4m2.

ISSN:3007-9640 DOI: https://doi.org/10.70114/acmsr.2025.3.1.P183

It can be seen that the motion process of m2 mainly consists of a collision stage and a non-collision stage. When m2 collides with the structure, the velocities of the particles and the structure before and after the collision can be obtained based on the definition of e and the conservation of momentum. That is

$$\dot{x}_{1+} = \dot{x}_{1-} + \frac{\mu(1+e)}{1+\mu}\dot{x}_{1-}, \tag{1}$$

$$\dot{x}_{2+} = -e\dot{x}_{2-}. \tag{2}$$

Here, $\dot{x}_{1-}$ and $\dot{x}_{1+}$ represent the relative velocities of the structure before and after the collision, respectively. $\dot{x}_{2-}$ and $\dot{x}_{2+}$ denote the relative velocities of the particle before and after the collision. μ = m2/m1 represents the particle's added mass ratio.

For non-collision stage, the motion state of the system can be obtained through the following motion equations.

$$\begin{cases} m_1(\ddot{x}_1+\ddot{x}_g)+c_1\dot{x}_1+k_1x_1=F_e \\ m_2(\ddot{x}_1+\ddot{x}_2+\ddot{x}_g)-F_e=0 \end{cases}, \tag{3}$$

where, Fe represents the control force between the particles and the structure during the non-collision stage. For the EISP model, Fe = 0. For the EISP-RF model, $F_e=m_2g\, f_r/r\, (\dot{x}_2/|\dot{x}_2|)$, where r is the particle radius. For the EISM model, $F_e=m_2gf_r/r\, (\dot{x}_2/|\dot{x}_2|)+q\ddot{x}_2$.

2.2 Full State Equivalent Single Particle Mechanics Model

To analyze the influence of the particle motion state on vibration reduction performance, an EWSM was established in which rolling and sliding of particles were considered, as shown in Fig. 2.

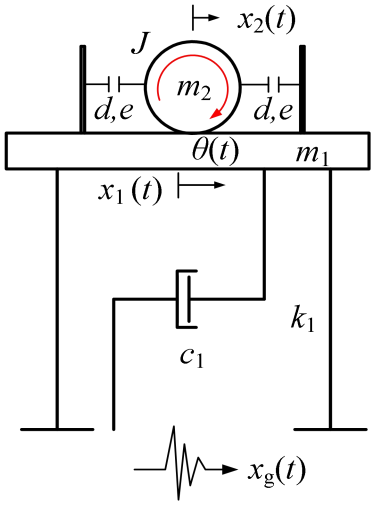

Fig. 2 EWSM

Here, J represents the rotational inertia of the particle, and θ (t) denotes the relative rotational angle of the particle. The motion process of the particle can also be divided into a non-collision phase and a collision phase.

In the non-collision stage, the motion states of the particles mainly include the stationary state, the pure rolling state and the rolling-sliding coupling state. The system motion equations for stationary state, rolling state and the rolling-sliding coupling state are given by Eqs. (2), (3), and (4), respectively, where fs represents the sliding friction coefficient.

$$\begin{cases} \ddot{x}_2=0 \\ m_2(\ddot{x}_1+\ddot{x}_2+\ddot{x}_g)+F_e=0 \quad s.t.|m_2(\ddot{x}_1+\ddot{x}_g)|<m_2g\dfrac{f_r}{r} \\ m_1(\ddot{x}_1+\ddot{x}_g)+c_1\dot{x}_1+k_1x_1=F_e \end{cases} \tag{4}$$

ISSN:3007-9640 DOI: https://doi.org/10.70114/acmsr.2025.3.1.P183

$$\begin{cases} m_2(\ddot{x}_1+\ddot{x}_2+\ddot{x}_g)+F_e=0 \\ F_e r-J\ddot{\theta}-m_2 g f_r \dot{x}_2/|\dot{x}_2|=0 \\ m_1(\ddot{x}_1+\ddot{x}_g)+c_1\dot{x}_1+k_1 x_1=F_e \\ \ddot{x}_2=\ddot{\theta}r \end{cases} \quad s.t. m_2 g\frac{f_r}{r}<F_e<m_2 g f_s \tag{5}$$

$$\begin{cases} m_2(\ddot{x}_1+\ddot{x}_2+\ddot{x}_g)+m_2 g f_s\dfrac{\dot{x}_2-\dot{\theta}r}{|\dot{x}_2-\dot{\theta}r|}=0 \\ m_1(\ddot{x}_1+\ddot{x}_g)+c_1\dot{x}_1+k_1 x_1=m_2 g f_s\dfrac{\dot{x}_2-\dot{\theta}r}{|\dot{x}_2-\dot{\theta}r|} \\ m_2 g f_s r\dfrac{\dot{x}_2-\dot{\theta}r}{|\dot{x}_2-\dot{\theta}r|}=J\ddot{\theta} \end{cases} \quad s.t. \quad \begin{matrix} \ddot{x}_2>\dfrac{m_2 g f_s r^2-r m_2 g f_r \dot{x}_2/|\dot{x}_2|}{J} \\ or \\ \dot{x}_2\neq\dot{\theta}r \end{matrix} \tag{6}$$

When particles collide with the structure, it is assumed that the collision occurs instantaneously. Both the energy dissipation caused by normal collision and the tangential collision induced by rolling are considered for EWSM. Additionally, it is assumed that the normal restitution coefficient en and the tangential restitution coefficient et are identical, i.e., en = et[13]. The vertical velocity of the particle resulting from the tangential collision is neglected. Based on the definition of e and the conservation of momentum,

$$\dot{x}_{1+}=\dot{x}_{1-}+\frac{\mu(1+e_n)}{1+\mu}\dot{x}_{1-}, \tag{7}$$

$$\dot{x}_{2+}=-e_n\dot{x}_{2-}, \tag{8}$$

$$\dot{\theta}_{+}=-e_t\dot{\theta}_{-}. \tag{9}$$

Here, - and + represent the relative angular velocities of the particle before and after the collision, respectively. The simulation flow of motion response for EWSM-SDOF under seismic excitation is shown in Fig. 3.

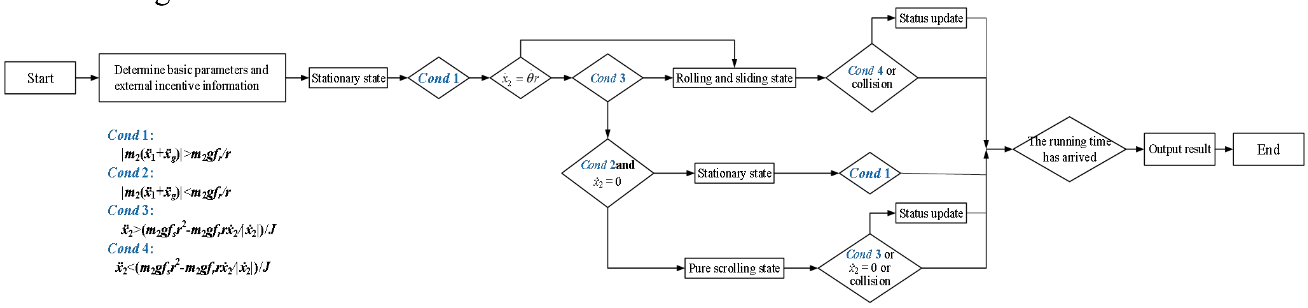

Fig. 3 Simulation process

The energy dissipation of the system can also be obtained. Where

$$D_f=\int m_2 g\frac{f_r}{r}sign(\dot{x}_2)[1-|sign(\dot{x}_2-\dot{\theta}r)|]dx_2+\int m_2 g f_s\, sign(\dot{x}_2-\dot{\theta}r)dx_2-\int m_2 g f_s r\, sign(\dot{x}_2-\dot{\theta}r)d\theta, \tag{10}$$

$$D_e=\sum_{\eta=1}^{n}\left\{\frac{1}{2}\frac{m_1 m_2}{m_1+m_2}(1-e_n^2)|\dot{x}_{2-}|^2\right\}, \tag{11}$$

$$D_{\mathrm{Re}}=\sum_{\eta=1}^{n}\left\{\frac{J}{2}\dot{\theta}_-^2(1-e_t^2)\right\}. \tag{12}$$

Df is the frictional dissipation energy of the particle, which is the sum of the rolling friction dissipation energy and the sliding friction dissipation energy. sign(x) is the sign function. De is the perpendicular collision dissipation energy. DRe is the tangential collision dissipation energy.

ISSN:3007-9640 DOI: https://doi.org/10.70114/acmsr.2025.3.1.P183

3. The Influence of Rquivalent Model on the Vibration Reduction Effect of Particle Dampers

To analyze the influence of different equivalent models on the vibration reduction performance of particle dampers, the numerical analysis was carried out under free vibration and harmonic excitation subsequently. The SDOF was selected as the controlled structure. The baseline parameter settings for the EWSM-SDOF as shown in Fig. 2 are shown in Table 1. The parameter settings corresponding to the other mechanical models are shown in Table 2, where the equivalent sliding mass model (ESMM) is the mechanical model that only considers sliding friction.

Tab. 1 Basic parameter settings

parameter	take a value
m_1 (kg)	17.96
k_1(N/m)	5400
c_1 (N·s/m)	8.1
μ (%)	6
e_n	0.25
e_t	0.25
d (m)	0.01
J	$0.4m_2r^2$
f_r (mm)	0.01
f_s	0.15

Tab. 2 Characteristic parameters corresponding to different mechanical models

model	e_n	e_t	J	f_r (mm)	f_s
EWSM	0.25	0.25	$0.4m_2r^2$	0.01	0.15
EISP	0.25	0	0	0	0
EISP-RF	0.25	0	0	0.01	∞
EISM	0.25	0.25	$0.4m_2r^2$	0.01	∞
ESMM	0.25	0	0	$0.15\times r$	∞

3.1 Under Free Vibration

The comparative analysis of the damping performance for different mechanical models under free vibration was carried out firstly. The initial displacement of the structure was set to 0.06 mm. The time-history curves of structural displacement are shown in Fig. 4. It can be obtained from the images that the particle dampers corresponding to the different mechanical models have a certain damping effect. The displacement amplitude decays rapidly in the initial stage and more slowly in the later stage. With the decrease of displacement amplitude, the concentrated mass m1 corresponding to the ESMM is less likely to produce relative motion due to the larger sliding friction, which results in the particle dampers cannot be effective in vibration reduction. In contrast, the particle dampers corresponding to other models demonstrate superior vibration reduction performance with relatively similar effectiveness.

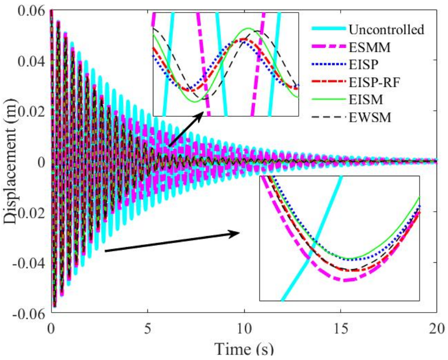

Fig. 4 Displacement response

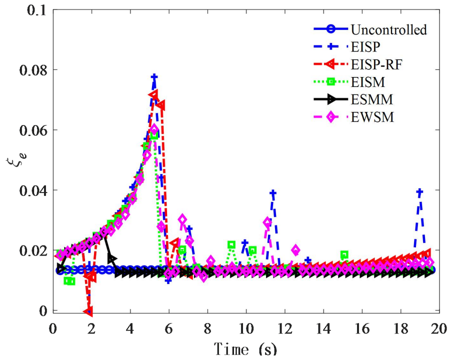

Fig. 5 ξ_e

ISSN:3007-9640 DOI: https://doi.org/10.70114/acmsr.2025.3.1.P183

To further quantify the energy dissipation capacity of the particle damper under free vibration, the damping ratio ξe of the structure with particle damper is statistically as shown in Fig. 5. The results indicate that the evolution of ξe under free vibration exhibits certain nonlinear characteristics. In the early stage of vibration, although the particle collision can generate large collision energy dissipation due to the large structural displacement, ξe is not ideal due to other nonlinear factors such as the momentum exchange and the impact phase angle. As the structure displacement response decreases, the particle collision state and momentum exchange gradually improve, which induces a gradual increase in ξe. When the relative motion of the particles is so small that they cannot collide with the structure, ξe suddenly decreases. The above analysis indicates that the vibration reduction performance of particle dampers under free vibration is significantly influenced by the structural displacement amplitude. It is worth noting that the particles of the ESMM model stop moving in the pre-motion phase and no longer play a vibration damping effect due to sliding friction. The vibration reduction effects corresponding to different mechanical models satisfy EISP > EISP-RF > EWSM > EISM > ESMM.

3.2 Under Harmonic Excitation

3.2.1 No collision stage

Based on the above analysis, it can be concluded that different mechanical models primarily influence the performance under non-collision astage. Therefore, the vibration reduction performance is initially analyzed under the assumption of no collisions. The excitation amplitude A is set to 0.02g. d is adjusted to be large enough to prevent the particles from colliding with the structure during movement. The root means square displacement amplification factor β of the structure relative to the ground motion is statistically calculated for different mechanical models, as shown in Fig. 6. In the figure, l1 represents the original structure's frequency response curve (FRC) of β and l2 represents the FRC after adding 6% additional mass. It can be observed that

(1) In the non-collision case, the interaction between the particle and the structure is small in both the EISP and EISP-RF models, which FRC overlap with the l1.

(2) For ESMM model, the sliding friction limits the motion of particles. The motion state of the structure with additional particles is equivalent to the response of the structure with the same mass attached, which FRC overlaps with l2.

(3) The EISM and EWSM models take into account the mass coupling effect caused by the particle rotation. The corresponding FRC are clearly located to the left of l1. When the β is large, sliding motion occurs in the EWSM model, which enhancing the energy dissipation capability of particles, as well as the vibration reduction performance. It is worth noting that in the ESMM model, the particles still do not undergo sliding motion when the β is large. Compared to pure sliding friction, the rolling-sliding mechanism in the EWSM model utilizes sliding friction more effectively for energy dissipation.

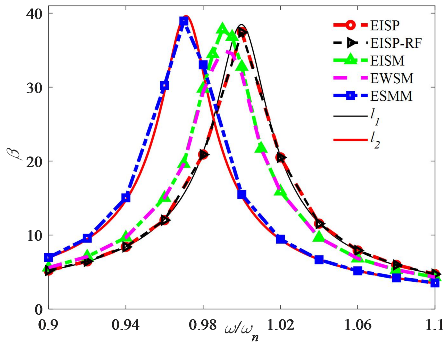

Fig.6 β under non-collision stage (A=0.02g)

ISSN:3007-9640 DOI: https://doi.org/10.70114/acmsr.2025.3.1.P183

After considering sliding friction, there is a significant nonlinear relationship between the interaction force Fe and the relative particle acceleration in both the EWSM and ESMM models. To further analyze the influence of A on the vibration reduction performance of different mechanical models, vibration reduction effect analyses are further conducted for different A, as shown in Fig. 7.

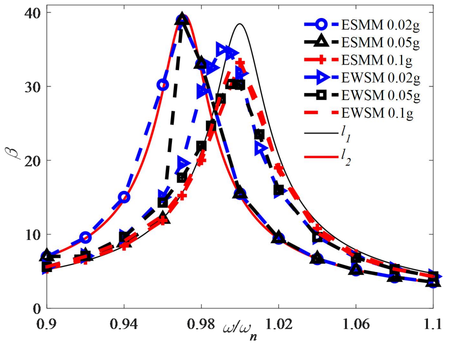

Fig.7 The influence of A on the vibration reduction effect during the non-collision stage

It can be obtained that

(1) For ESMM, the FRC of displacement overlaps with l2 when A is small. As A increases, the FRC gradually shifts toward l1. When A = 0.05g and the excitation frequency is low, the relative acceleration of the particle is high, which resulting in relative motion between the particle and the structure. In this case, energy dissipation and vibration reduction primarily through the action of sliding friction. At higher excitation frequencies, the relative acceleration between particle and strcuture decreases, which hindering the relative motion between particle and structure. The particles still mainly act as an additional mass. When A= 0.1g, the relative acceleration of the particle becomes significant. The structural FRC converges to curve l1. However, due to sliding friction, the particle damper exhibits a certain degree of vibration reduction.

(2) For EWSM, the FRC gradually shifts from the left toward l1 with the increasing of A. When A = 0.1g, the FRC of the EWSM nearly coincides with that of the ESMM. The nonlinear performance of the EWSM mechanical model due to sliding friction is improved after considering particle rolling compared to the ESMM model.

3.2.2 Collision stage

In order to comparatively analyze the performance of particle damper after collision, d is set to 0.01m. A comparative analysis of vibration reduction performance under resonant harmonic excitation was conducted. The time-history curve of the relative structural displacement is shown in Fig. 8. The relative displacement x2 is shown in Fig. 9. The development of collision energy dissipation with time is shown in Fig. 10.

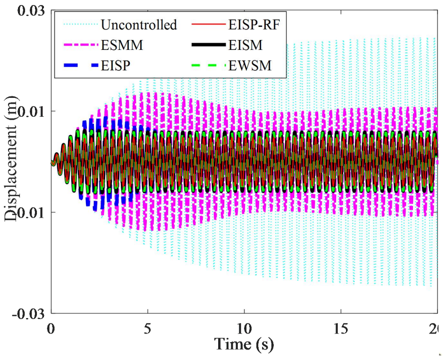

Fig. 8 Relative displacement of structure

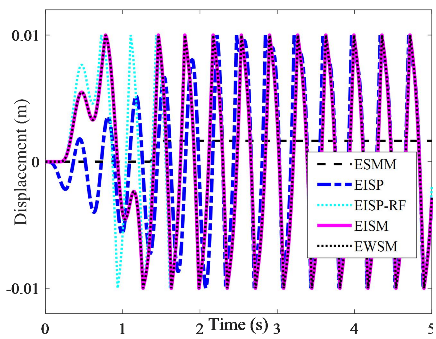

Fig. 9 Relative displacement of particles

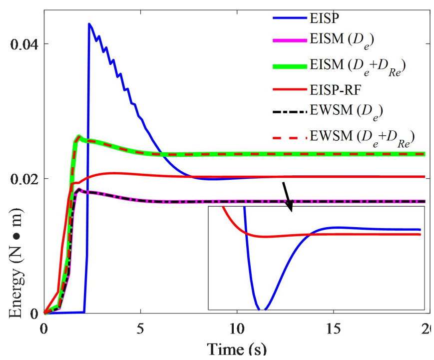

Fig. 10 Collision energy dissipation

ISSN:3007-9640 DOI: https://doi.org/10.70114/acmsr.2025.3.1.P183

It can be seen that all the mechanical models have a significant damping performance. A detailed analysis is provided as below.

(1) Compared to the uncontrolled structure, the steady-state vibration reduction effects for the EISP, EISP-RF, EWSM, EISM, and ESMM models are 80.45%, 80.37%, 76.26%, 76.26%, and 56.50%, respectively. The EISP corresponds to the best damping effect, while the ESMM corresponds to the worst damping effect.

(2) It can be seen from the particle relative displacement time course curves that it is more difficult for a single particle in the ESMM to slide due to high sliding friction. Therefore, the particles only play the role of additional mass. By combining the change rule of the structural FRC with the additional mass, it can be seen that the ESMM has a certain damping effect at the resonance frequency, but it is not ideal.

(3) A comparative analysis of the EISM and EWSM models shows that, the particles in EWSM model are less likely to produce sliding under the current A. Therefore, the time-displacement curve of the particle corresponding to the EWSM overlaps with that of the EISM model. Compared to the EISP model, although the total energy dissipation during collision (De+DRe) is higher in the EISM and EWSM models, the effective collision energy dissipation (De) is smaller. Additionally, there exist mass coupling effects caused by rolling. Therefore, the damping effect is slightly lower than the EISP model.

(4) The comparison between the EISP-RF model and the EISP model indicates that rolling friction has little effect on the displacement response of the structure in steady state. After considering rolling friction, the collision energy dissipation in the steady state slightly decreases, and the vibration reduction effect slightly diminishes. However, rolling friction has little effect on damping performance overall.

(5) It is worth noting that the start-up times of EISP-RF, EISM and EWSM are shorter compared to the EISP model under the assumption that the particles are initially located in the center of the container. The interaction between the particle and the structure, like rolling friction and inertia coupling, in the non-collision stage facilitates collision between the particle and the structure.

For dampers with impact effects, it is worth noting that the effects of A and d on the damping effect are coupled to each other due to the existence of d [14]. Therefore, an analysis of the influence of A is conducted under the condition of adjusting d to ensure that the d /A =0.5 m/g as shown in Fig. 11. It can be seen that the damping effects of EISP, EISP-RF and EISM remain basically unchanged with the increase of A when d /A is kept constant. In contrast, as A increases, the corresponding damping effects of EWSM and ESMM gradually increase due to the sliding friction. Moreover, when A is larger, the damping effects of EWSM and ESMM gradually approach the damping effects of EISP.

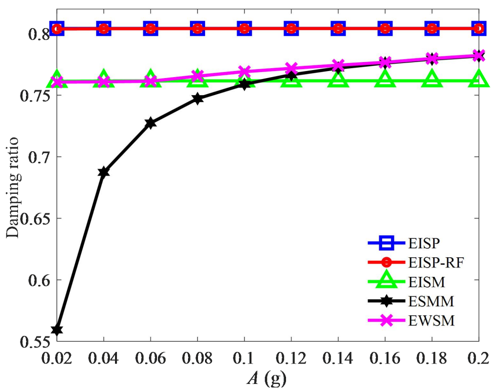

Fig.11 The influence of A on the vibration reduction effect under d /A =0.5 m/g

3.3 Under Seismic Excitation

El Center, Kobe and Taft seismic records were selected as ground inputs to compare the damping performance of different mechanical models under seismic effects. The peak ground

ISSN:3007-9640 DOI: https://doi.org/10.70114/acmsr.2025.3.1.P183

acceleration (PGA) was set to 0.2 g. The values of structural and mechanical model parameters are the same as in Tables 1 and 2. The analysis results show that the particle dampers of the different mechanical models have certain damping effects. The statistics of structural response eigenvalues are shown in Fig. 12. The maximum displacement response damping ratio and the root-mean-square displacement RMS damping ratio of the structure are shown in Fig. 12(a). The effect of the model on the collision energy dissipation De is shown in Fig. 12(b). The effect of the model on the friction dissipation energy Df is shown in Fig. 12(c).

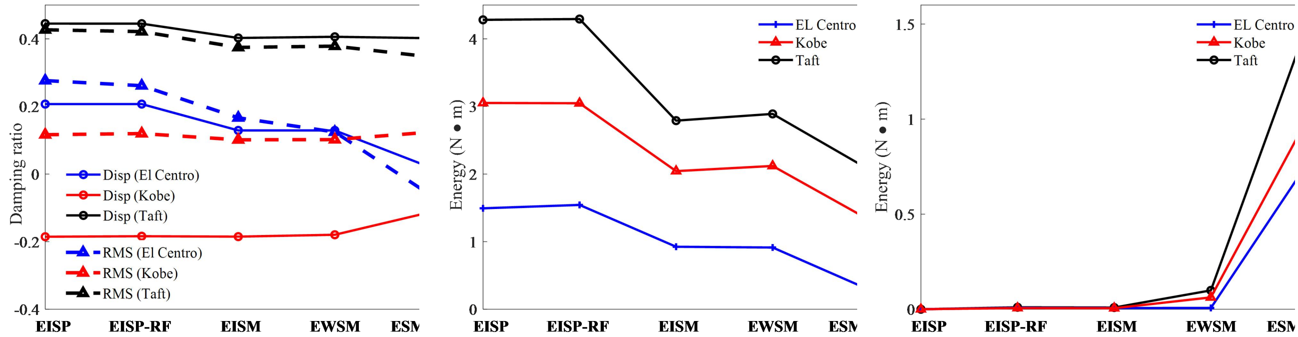

(a) Damping ratio (b) D_e (c) D_f

Fig. 12 Eigenvalue statistics

It can be seen from Fig. 15 that there is a certain difference in the vibration damping effect of particle dampers corresponding to different models under different assumption conditions. The details are as follows.

(1) Due to the variability of seismic records, there are some differences in the variation rules of vibration damping effects corresponding to different mechanical models. The vibration damping effect generally satisfies EISP > EISP-RF > EWSM > EISM > ESMM.

(2) EISP and EISP-RF have the best and similar damping effects. However, due to the differences in seismic spectral characteristics, there are differences in the patterns of rolling friction effects on the damping performance. After considering the effect of rolling friction, De and Df are also changed.

(3) The EISM and EWSM models further consider the inertia effect caused by the particle rotation on the basis of EISP. After considering the inert effect, on the one hand, the particle motion state is changed. The advective kinetic energy of the particles decreases, as well as the vertical collision energy dissipation De between the particles and the structure. The corresponding damping effect is reduced. On the other hand, the mass coupling effect due to the inert effect also has an effect on the damping performance. Under the influence of the above factors, the damping effect of EISM and EWSM is reduced compared to EISP and EISP-RF after considering the effect of inerter. EWSM further considers the effect of sliding friction compared to EISM. Sliding friction improves the particle motion and enhances the frictional energy dissipation between the particles and the structure. Therefore, the particle damper damping effect is enhanced after considering sliding friction.

(4) ESMM enhances the friction coefficient compared to the EISP-RF model. The sliding friction between the particles and the structure restricts the relative motion of the particles and therefore reduces the collision energy dissipation between the particles and the structure. However, the frictional energy dissipation between particles and structures is further increased as a result. Due to the difference in seismicity, the damping effect is significantly reduced under El Center and Taft action. However, the damping effect is increased in Kobe.

ISSN:3007-9640 DOI: https://doi.org/10.70114/acmsr.2025.3.1.P183

4. Summary

In this study, the EWSM model is proposed, as well as the corresponding numerical simulation method. Based on this, the influence of different equivalent mechanical models on the vibration reduction performance is conducted. The main conclusions are as follows.

(1) The vibration reduction performance analysis under free vibration indicates that the performance of the single particle damper is significantly influenced by the structural displacement amplitude. As the displacement amplitude decreases, the ESMM model becomes inactive.

(2) The comparative analysis of vibration reduction performance under harmonic excitation shows that when the particles do not collide with the structure, there is no interaction between the particles and the structure for the EISP and EISP-RF models. Therefore, the corresponding frequency response curve is consistent with the curve of the original structure. In the ESMM model, no relative motion occurs between the particles and the structure, causing its frequency response curve to coincide with l2. Due to the mass transfer effect caused by the inerter effect, the frequency response curves of the EISM and EWSM models lie between l1 and l2 with a slight improvement in vibration reduction after considering sliding friction. The analysis of the impact of A during the non-collision phase indicates that A has a significant effect on the vibration reduction performance of the model. After particle collisions occur (d = 0.01m), due to the rolling-inertia-sliding mechanism, the vibration reduction effect is improved compared to pure sliding. The influence of A on vibration reduction performance shows that the vibration reduction performance of EISP, EISP-RF and EISM remains relatively unchanged with the increase of A. However, the collision energy dissipation in the EWSM and ESMM models gradually increases, which resulting in a corresponding improvement in vibration damping performance.

(3) Under seismic excitation, the vibration reduction performance of EISP > EISP-RF > EWSM > EISM > ESMM. The comparison between the EISP-RF and EISP models indicates that the rolling friction have little effect on the performance of particles. After considering the inertial effect, the vibration reduction performance of EISM and EWSM models significantly decreases due to mass coupling and motion state coupling. It is important to note that, as EWSM further considers sliding friction, it forms a rolling-sliding transition mechanism, which benefits from sliding friction and improves vibration reduction performance. The particles in the ESMM model are harder to vibrate due to the larger sliding friction.

References

[1] Papalou A, Masri SF. An experimental investigation of particle dampers under harmonic excitation [J]. Journal of Vibration and Control, 1998, 4(4): 361-379.

[2] Lu Zheng, Wang Dianchao, Lv Xilin. Comparative experimental study of particle damper and tuned mass damper[J]. Earthouake Engineering and Engineering Dynamics, 2014, 34 (S1): 738-742. (in Chinese)

[3] Yin ZJ, Su F, Zhang H. Investigation of the energy dissipation of different rheology behaviors in a non-obstructive particle damper [J]. Powder Technology, 2017, 321: 270-275.

[4] Asakura T. Vibroacoustic damping effect of particles on double-plate structures [J]. Applied Acoustics, 2022, 197: 108920.

[5] Wei Shoubei. Study of vibration reduction structure dampingcharacteristics with particle damper based on SVR[D]. Jiangsu University of Science and Technology, 2016. (in Chinese)

[6] Wu Chengjun, Yang Ruichao, Wang Dongqiang. Prediction on Vibration Response of Cantilever Particle-damping Beam Based on Two-phase Flow Theory of Gas-particle [J] Journal of Mechanical Engineering, 2013, 49 (10): 53-61. (in Chinese)

[7] Yao B, Chen Q, Xiang HY, et al. Experimental and theoretical investigation on dynamic properties of tuned particle damper [J]. International Journal of Mechanical Sciences, 2014, 80: 122-130.

[8] Lu Zheng, Chen Xiaoyi, Wang Dianchao, et al. Numerical simulation for vibration reductioncontrol of particle tuned mass dampers [J]. Journal of Vibration and Shock, 2017, 36 (03): 46-50. (in Chinese)

ISSN:3007-9640 DOI: https://doi.org/10.70114/acmsr.2025.3.1.P183
[9] Wang Baoshun, He Haoxiang, Yan Weiming. Analytical Model and Optimization Analysis of Combineddamping System with TMD and Particle Damper [J]. Engineering Mechanics, 2021, 38 (06): 191-208. (in Chinese)

[10] Lu Z, Chen XY, Zhou Y. An equivalent method for optimization of particle tuned mass damper based on experimental parametric study [J]. Journal of Sound and Vibration, 2018, 419: 571-584.

[11] Yan WM, Wang BS, He HX. Research of mechanical model of particle damper with friction effect and its experimental verification [J]. Journal of Sound and Vibration, 2019, 460: 114898.

[12] Huang XH, Li XJ, Wang J. Optimal design of inerter‐based nonpacked particle damper considering particle rolling [J]. Earthquake Engineering & Structural Dynamics, 2021, 50(7): 1908-1930.

[13] Kondic L. Dynamics of spherical particles on a surface: collision-induced sliding and other effects [J]. Phys Rev E Stat Phys Plasmas Fluids Relat Interdiscip Topics, 1999, 60(1): 751-770. eng

[14] Huang XH, Xu WB, Yan WM, et al. Equivalent model and parameter analysis of non-packed particle damper [J]. Journal of Sound and Vibration, 2021, 491: 115775.